



EUROPEAN ORGANIZATION FOR NUCLEAR RESEARCH

CERN-EP/90-44

4 April 1990

SEARCH FOR LIGHT NEUTRAL HIGGS PARTICLES PRODUCED IN Z^0 DECAYS

DELPHI Collaboration

Abstract

A search for the neutral Higgs boson in Z^0 decays has been performed using the DELPHI detector at the Large Electron Positron collider (LEP) at CERN. We looked for the decay of Z^0 into a neutral Higgs particle and a pair of fermions. No events fulfilled the criteria for H^0 production. Our results, which are based on an integrated luminosity of 530 nb^{-1} , exclude a minimal Standard Model Higgs boson with a mass in the range $210 \text{ MeV}/c^2$ to $14 \text{ GeV}/c^2$ at 95% confidence level.

- P. Abreu¹⁶⁾, W. Adam³⁷⁾, F. Adami²⁸⁾, T. Adye²⁷⁾, G. D. Alekseev¹²⁾, J. V. Allaby⁷⁾, P. Allen³⁶⁾,
 S. Almedhed¹⁹⁾, F. Alted³⁶⁾, S. J. Alvsvaag⁴⁾, U. Amaldi⁷⁾, E. Anassontzis³⁾, W. D. Apel¹³⁾, B. Asman³²⁾,
 C. Astor Ferreres³⁰⁾, J. E. Augustin¹⁵⁾, A. Augustinus⁷⁾, P. Baillon⁷⁾, P. Bambade¹⁵⁾, F. Barao¹⁶⁾,
 G. Barbiellini³⁴⁾, D. Yu. Bardin¹²⁾, A. Baroncelli²⁹⁾, O. Barring¹⁹⁾, W. Bartl³⁷⁾, M. J. Bates²⁵⁾,
 M. Baubillier¹⁸⁾, K. H. Becks³⁹⁾, C. J. Beeston²⁵⁾, P. Beilliere⁶⁾, I. Belokopytov³¹⁾, P. Beltran⁹⁾, D. Benedic⁸⁾,
 J. M. Benloch³⁶⁾, M. Berggren³²⁾, D. Bertrand²⁾, S. Biagi¹⁷⁾, F. Bianchi³³⁾, J. H. Bibby²⁵⁾, M. S. Bilenky¹²⁾,
 P. Billoir¹⁸⁾, J. Bjarne¹⁹⁾, D. Bloch⁸⁾, P. N. Bogolubov¹²⁾, D. Bollini⁵⁾, T. Bolognese²⁸⁾, M. Bonapart²²⁾,
 P. S. L. Booth¹⁷⁾, M. Boratav¹⁸⁾, P. Borgeaud²⁸⁾, H. Borner²⁵⁾, C. Bosio²⁹⁾, O. Botner³⁵⁾, B. Bouquet¹⁵⁾,
 M. Bozzo¹⁰⁾, S. Braibant⁷⁾, P. Branchini²⁹⁾, K. D. Brand³⁹⁾, R. A. Brenner¹¹⁾, C. Bricman²⁾, R. C. A. Brown⁷⁾,
 N. Brummer²²⁾, J. M. Brunet⁶⁾, L. Bugge²⁴⁾, T. Buran²⁴⁾, H. Burmeister⁷⁾, C. M. Buttar²⁵⁾,
 J. A. M. A. Buytaert²⁾, M. Caccia²⁰⁾, M. Calvi²⁰⁾, A. J. Camacho Rozas³⁰⁾, J. E. Campagne⁷⁾, A. Champion¹⁷⁾,
 T. Camporesi⁷⁾, V. Canale²⁹⁾, F. Cao²⁾, L. Carroll¹⁷⁾, C. Caso¹⁰⁾, E. Castelli³⁴⁾, M. V. Castillo Gimenez³⁶⁾,
 A. Cattai⁷⁾, F. R. Cavallo⁵⁾, L. Cerrito²⁹⁾, P. Charpentier⁷⁾, P. Checchia²⁶⁾, G. A. Chelkov¹²⁾, L. Chevalier²⁸⁾,
 P. V. Chliapnikov³¹⁾, V. Chorowicz¹⁸⁾, R. Cirio³³⁾, M. P. Clara³³⁾, J. L. Contreras³⁶⁾, R. Contri¹⁰⁾,
 G. Cosme¹⁵⁾, F. Couchot¹⁵⁾, H. B. Crawley¹⁾, D. Crennell²⁷⁾, M. Cresti²⁶⁾, G. Crosetti¹⁰⁾, N. Crosland²⁵⁾,
 M. Crozon⁶⁾, J. Cuevas Maestro³⁰⁾, S. Czellar¹¹⁾, S. Dagoret¹⁵⁾, E. Dahl-Jensen²¹⁾, B. D'Almagne¹⁵⁾,
 M. Dam⁷⁾, G. Damgaard²¹⁾, G. Darbo¹⁰⁾, E. Daubie²⁾, M. Davenport⁷⁾, P. David¹⁸⁾, A. De Angelis³⁴⁾,
 M. De Beer²⁸⁾, H. De Boeck²⁾, W. De Boer¹³⁾, C. De Clercq²⁾, M. D. M. De Fez Laso³⁶⁾, N. De Groot²²⁾,
 C. De La Vaissiere¹⁸⁾, B. De Lotto³⁴⁾, C. Defoix⁶⁾, D. Delikaris⁷⁾, P. Delpierre⁶⁾, N. Demaria³³⁾,
 K. G. Denisenko¹²⁾, L. Di Ciaccio²⁹⁾, A. N. Diddens²²⁾, H. Dijkstra⁷⁾, F. Djama⁸⁾, J. Dolbeau⁶⁾, K. Doroba³⁸⁾,
 M. Dracos⁸⁾, J. Drees³⁹⁾, M. Dris²³⁾, W. Dulinski⁸⁾, R. Dzhelyadin³¹⁾, D. N. Edwards¹⁷⁾, L. O. Eek³⁵⁾,
 P. A. M. Eerola¹¹⁾, T. Ekelof³⁵⁾, G. Ekspong³²⁾, J. P. Engel⁸⁾, V. Falaleev³¹⁾, A. Fenyuk³¹⁾,
 M. Fernandez Alonso³⁰⁾, A. Ferrer³⁶⁾, S. Ferroni¹⁰⁾, T. A. Filippas²³⁾, A. Firestone¹⁾, H. Foeth⁷⁾,
 E. Fokitis²³⁾, F. Fontanelli¹⁰⁾, H. Forsbach³⁹⁾, B. Franek²⁷⁾, K. E. Fransson³⁵⁾, P. Frenkiel⁶⁾, D. C. Fries¹³⁾,
 R. Fruhwirth³⁷⁾, F. Fulda-Quenzer¹⁵⁾, H. Fuerstenau¹³⁾, J. Fuster⁷⁾, J. M. Gago¹⁶⁾, G. Galeazzi²⁶⁾,
 D. Gamba³³⁾, U. Gasparini²⁶⁾, P. Gavillet⁷⁾, S. Gawne¹⁷⁾, E. N. Gazis²³⁾, P. Giacomelli⁵⁾, K. W. Glitza³⁹⁾,
 R. Gokiel¹⁸⁾, V. M. Golovatyuk¹²⁾, A. Goobar³²⁾, G. Gopal²⁷⁾, M. Gorski³⁸⁾, V. Gracco¹⁰⁾, A. Grant⁷⁾,
 F. Grard²⁾, E. Graziani²⁹⁾, M. H. Gros¹⁵⁾, G. Grosdidier¹⁵⁾, B. Grossetete¹⁸⁾, S. Gumenyuk³¹⁾, J. Guy²⁷⁾,
 F. Hahn³⁹⁾, M. Hahn¹³⁾, S. Haider⁷⁾, Z. Hajduk¹⁴⁾, A. Hakansson¹⁹⁾, A. Hallgren³⁵⁾, K. Hamacher³⁹⁾,
 G. Hamel De Monchenault²⁸⁾, J. F. Harris²⁵⁾, B. Heck⁷⁾, I. Herbst³⁹⁾, J. J. Hernandez³⁶⁾, P. Herquet²⁾,
 H. Herr⁷⁾, E. Higon³⁶⁾, H. J. Hilke⁷⁾, T. Hofmohl³⁸⁾, R. Holmes¹⁾, S. O. Holmgren³²⁾, J. E. Hooper²¹⁾,
 M. Houlden¹⁷⁾, J. Hrubec³⁷⁾, P. O. Hulth³²⁾, K. Hultqvist³²⁾, D. Husson⁸⁾, B. D. Hyams⁷⁾, P. Ioannou³⁾,
 P. S. Iversen⁴⁾, J. N. Jackson¹⁷⁾, P. Jalocha¹⁴⁾, G. Jarlskog¹⁹⁾, P. Jarry²⁸⁾, B. Jean-Marie¹⁵⁾,
 E. K. Johansson³²⁾, M. Jonker⁷⁾, L. Jonsson¹⁹⁾, P. Juillot⁸⁾, R. B. Kadyrov¹²⁾, V. G. Kadyshesky¹²⁾,
 G. Kalkanis³⁾, G. Kalmus²⁷⁾, G. Kantardjian⁷⁾, F. Kapusta¹⁸⁾, P. Kapusta¹⁴⁾, S. Katsanevas³⁾,
 E. C. Katsoufis²³⁾, R. Keranen¹¹⁾, J. Kesteman²⁾, B. A. Khomenko¹²⁾, B. King¹⁷⁾, H. Klein⁷⁾, W. Klempt⁷⁾,
 A. Klovning⁴⁾, P. Kluit²⁾, J. H. Koehne¹³⁾, B. Koene²²⁾, P. Kokkinias⁹⁾, M. Kopf¹³⁾, M. Koratzinos⁷⁾,
 K. Korcyl¹⁴⁾, B. Korzen⁷⁾, C. Kourkoumelis³⁾, T. Kreuzberger³⁷⁾, J. Krolikowski³⁸⁾, U. Krueener-Marquis³⁹⁾,
 W. Krupinski¹⁴⁾, W. Kucewicz²⁰⁾, K. Kurvinen¹¹⁾, M. I. Laakso¹¹⁾, C. Lambropoulos⁹⁾, J. W. Lamsa¹⁾,
 L. Lanceri³⁴⁾, V. Lapchine³¹⁾, V. Lapin³¹⁾, J. P. Laugier²⁸⁾, R. Lauhakangas¹¹⁾, P. Laurikainen¹¹⁾,
 G. Leder³⁷⁾, F. Ledroit⁶⁾, J. Lemonne²⁾, G. Lenzen³⁹⁾, V. Lepeltier¹⁵⁾, A. Letessier-Selvon¹⁸⁾, E. Lieb³⁹⁾,
 E. Lillestol⁷⁾, E. Lillethun⁴⁾, J. Lindgren¹¹⁾, I. Lippi²⁶⁾, R. Llosa³⁶⁾, B. Loerstad¹⁹⁾, M. Lokajicek¹²⁾,
 J. G. Loken²⁵⁾, A. Lopez¹⁵⁾, M. A. Lopez Aguera³⁰⁾, D. Loukas⁹⁾, J. J. Lozano³⁶⁾, R. Lucock²⁷⁾,
 B. Lund-Jensen³⁵⁾, P. Lutz⁶⁾, L. Lyons²⁵⁾, G. Maehlum⁷⁾, A. Maltezos⁹⁾, F. Mandl³⁷⁾, J. Marco³⁰⁾,
 J. C. Marin⁷⁾, A. Markou⁹⁾, L. Mathis⁶⁾, C. Matteuzzi²⁰⁾, G. Matthiae²⁹⁾, M. Mazzucato²⁶⁾,
 M. Mc Cubbin¹⁷⁾, R. Mc Kay¹⁾, E. Menichetti³³⁾, C. Meroni²⁰⁾, W. T. Meyer¹⁾, W. A. Mitaroff³⁷⁾,
 G. V. Mitselmakher¹²⁾, U. Mjoernmark¹⁹⁾, T. Moa³²⁾, R. Moeller²¹⁾, K. Moenig³⁹⁾, M. R. Monge¹⁰⁾,
 P. Morettini¹⁰⁾, H. Mueller¹³⁾, H. Muller⁷⁾, G. Myatt²⁵⁾, F. Naraghi¹⁸⁾, U. Nau-Korzen³⁹⁾, F. L. Navarria⁵⁾,
 P. Negri²⁰⁾, B. S. Nielsen²¹⁾, M. Nigro²⁶⁾, V. Nikolaenko³¹⁾, V. Obraztsov³¹⁾, R. Orava¹¹⁾, A. Ouraou²⁸⁾,
 R. Pain¹⁸⁾, K. Pakonski¹⁴⁾, H. Palka¹⁴⁾, T. Papadopoulou²³⁾, L. Pape⁷⁾, P. Pasini⁵⁾, A. Passeri²⁹⁾,
 M. Pegoraro²⁶⁾, V. Perevozchikov³¹⁾, M. Pernicka³⁷⁾, M. Pimenta¹⁶⁾, O. Pingot²⁾, C. Pinori²⁶⁾, A. Pinsent²⁵⁾,
 M. E. Pol¹⁶⁾, B. Poliakov³¹⁾, G. Polok¹⁴⁾, P. Poropat³⁴⁾, V. N. Pozdniakov¹³⁾, P. Privitera⁵⁾, A. Pullia²⁰⁾,
 J. Pyyhtia¹¹⁾, A. A. Rademakers²²⁾, D. Radojicic²⁵⁾, S. Ragazzi²⁰⁾, W. H. Range¹⁷⁾, P. N. Ratoff²⁵⁾,
 A. L. Read²⁴⁾, N. G. Redaelli²⁰⁾, M. Regler³⁷⁾, D. Reid¹⁷⁾, P. B. Renton²⁵⁾, L. K. Resvanis³⁾, F. Richard¹⁵⁾,
 J. Ridky¹³⁾, G. Rinaudo³³⁾, I. Roditi⁷⁾, A. Romero³³⁾, P. Ronchese²⁶⁾, E. Rosenberg¹⁾, U. Rossi⁵⁾, E. Rosso⁷⁾,
 P. Roudeau¹⁵⁾, T. Rovelli⁵⁾, V. Ruhlmann²⁸⁾, A. Ruiz³⁰⁾, H. Saarikko¹¹⁾, D. Sacco²⁹⁾, Y. Sacquin²⁸⁾,
 E. Sanchez³⁶⁾, E. Sanchis³⁶⁾, M. Sannino¹⁰⁾, M. Schaeffer⁸⁾, H. Schneider¹³⁾, F. Scuri³⁴⁾, A. Sebastia³⁶⁾,
 Yu. N. Sedych¹²⁾, A. M. Segar²⁵⁾, R. Sekulin²⁷⁾, M. Sessa³⁴⁾, G. Sette¹⁰⁾, R. Seufert¹³⁾, R. C. Shellard⁷⁾,

P.Siegrist²⁸⁾, S.Simonetti¹⁰⁾, F.Simonetto²⁶⁾, T.B.Skaali²⁴⁾, J.Skeens¹⁾, G.Skjevling²⁴⁾, G.Smadja²⁸⁾, N.E.Smirnov³¹⁾, G.R.Smith²⁷⁾, R.Sosnowski³⁸⁾, K.Spang²¹⁾, E.Spiriti²⁹⁾, S.Squarcia¹⁰⁾, H.Staeck³⁹⁾, C.Stanescu²⁹⁾, G.Stavropoulos⁹⁾, F.Stichelbaut²⁾, A.Stocchi²⁰⁾, J.Strauss³⁷⁾, R.Strub⁸⁾, C.Stubenrauch⁷⁾, M.Szczekowski³⁸⁾, M.Szeptycka³⁸⁾, P.Szymanski³⁸⁾, S.Tavernier²⁾, G.Theodosiou⁹⁾, A.Tilquin⁶⁾, J.Timmermans²²⁾, V.G.Timofeev¹²⁾, L.G.Tkatchev¹²⁾, T.Todorov¹²⁾, D.Z.Toet²²⁾, A.K.Toppol⁴⁾, L.Tortora²⁹⁾, D.Treille⁷⁾, U.Trevisan¹⁰⁾, G.Tristram⁶⁾, C.Troncon²⁰⁾, E.N.Tsyganov¹²⁾, M.Turala¹⁴⁾, R.Turchetta⁸⁾, M.L.Turluer²⁸⁾, T.Tuuva¹¹⁾, I.A.Tyapkin¹²⁾, M.Tyndel²⁷⁾, S.Tzamarias⁷⁾, F.Udo²²⁾, S.Ueberschaer³⁹⁾, V.A.Uvarov³¹⁾, G.Valenti⁵⁾, E.Vallazza³³⁾, J.A.Valls³⁶⁾, G.W.Van Apeldoorn²²⁾, P.Van Dam²²⁾, W.K.Van Doninck²⁾, N.Van Eijndhoven⁷⁾, C.Vander Velde²⁾, J.Varela¹⁶⁾, P.Vaz¹⁶⁾, G.Vegni²⁰⁾, M.E.Veitch³⁵⁾, E.Vela³⁶⁾, J.Velasco³⁶⁾, L.Ventura²⁶⁾, W.Venus²⁷⁾, F.Verbeure²⁾, L.Vibert¹⁸⁾, D.Vilanova²⁸⁾, E.V.Vlasov³¹⁾, A.S.Vodopianov¹²⁾, M.Vollmer³⁹⁾, G.Voulgaris³⁾, M.Voutilainen¹¹⁾, V.Vrba¹²⁾, H.Wahlen³⁹⁾, C.Walck³²⁾, F.Waldner³⁴⁾, M.Wayne¹⁾, P.Weilhammer⁷⁾, J.Werner³⁹⁾, A.M.Wetherell⁷⁾, J.H.Wickens²⁾, J.Wikne²⁴⁾, W.S.C.Williams²⁵⁾, M.Winter⁸⁾, D.Wormald²⁴⁾, G.Wormser¹⁵⁾, K.Woschnagg³⁵⁾, N.Yamdagni³²⁾, P.Yepes²²⁾, A.Zaitsev³¹⁾, A.Zalewska¹⁴⁾, P.Zalewski³⁸⁾, E.Zevgolatakos⁹⁾, G.Zhang³⁹⁾, N.I.Zimin¹²⁾, R.Zitoun¹⁸⁾, R.Zukanovich Funchal⁶⁾, G.Zumerle²⁶⁾, J.Zuniga³⁶⁾

(Submitted to Nuclear Physics B)

- ¹⁾Ames Laboratory and Department of Physics, Iowa State University, AMES IA 50011, U. S. A.
²⁾Physics Department, Univ. Instelling Antwerpen, Universiteitsplein 1, B-2610 WILRIJK.
 IIHE, ULB-VUB, Pleinlaan 2, B-1050 BRUXELLES.
 Service de Phys. des Part. Elém., Faculté des Sciences, Université de l'Etat Mons, Av. Maistriau 19, B-7000 MONS.
³⁾Physics Laboratory, University of Athens, Solonos Str. 104, GR-10680 ATHENS.
⁴⁾Department of Physics, University of Bergen, Allégaten 55, N-5007 BERGEN.
⁵⁾Dipartimento di Fisica, Università di Bologna and INFN, Via Irnerio 46, I-40126 BOLOGNA.
⁶⁾Collège de France, Lab. de Physique Corpusculaire, 11 pl. M. Berthelot, F-75231 PARIS CEDEX 5.
⁷⁾CERN, CH-1211 GENEVA 23.
⁸⁾Division des Hautes Energies, CRN - Groupe DELPHI, B.P. 20 CRO, F-67037 STRASBOURG CEDEX.
⁹⁾Greek Atomic Energy Commission, Nucl. Research Centre Demokritos, P.O. Box 60228, GR-15310 AGHIA PARASKEVI.
¹⁰⁾Dipartimento di Fisica, Università di Genova and INFN, Via Dodecaneso 33, I-16146 GENOVA.
¹¹⁾Dept. of High Energy Physics, University of Helsinki, Siltavuorenpenger 20 C, SF-00170 HELSINKI 17.
¹²⁾Joint Institute for Nuclear Research, Dubna, Head Post Office, P.O. Box 79, 101 000 MOSCOW, U.R.S.S.
¹³⁾Institut für Experimentelle Kernphysik, Universität Karlsruhe, Postfach 6980, D-7500 KARLSRUHE 1.
¹⁴⁾High Energy Physics Laboratory, Institute of Nuclear Physics, Ul. Kawiora 26 a, PL-30055 KRAKOW 30.
¹⁵⁾Université de Paris-Sud, Lab. de l'Accélérateur Linéaire, Bat 200, F-91405 ORSAY.
¹⁶⁾LIP, Av. Elias Garcia 14 - 1e, P-1000 LISBOA CODEX.
¹⁷⁾Department of Physics, University of Liverpool, P.O. Box 147, GB - LIVERPOOL L69 3BX.
¹⁸⁾LPNHE, Universités Paris VI et VII, Tour 33 (RdC), 4 place Jussieu, F-75230 PARIS CEDEX 05.
¹⁹⁾Department of Physics, University of Lund, Sölvegatan 14, S-22363 LUND.
²⁰⁾Dipartimento di Fisica, Università di Milano and INFN, Via Celoria 16, I-20133 MILANO.
²¹⁾Niels Bohr Institute, Blegdamsvej 17, DK-2100 COPENHAGEN 0.
²²⁾NIKHEF-H, Postbus 41882, NL-1009 DB AMSTERDAM.
²³⁾National Technical University, Physics Department, Zografou Campus, GR-15773 ATHENS.
²⁴⁾Physics Department, University of Oslo, Blindern, N-1000 OSLO 3.
²⁵⁾Nuclear Physics Laboratory, University of Oxford, Keble Road, GB - OXFORD OX1 3RH.
²⁶⁾Dipartimento di Fisica, Università di Padova and INFN, Via Marzolo 8, I-35131 PADOVA.
²⁷⁾Rutherford Appleton Laboratory, Chilton, GB - DIDCOT OX11 0QX.
²⁸⁾CEN-Saclay, DPhPE, F-91191 GIF-SUR-YVETTE CEDEX.
²⁹⁾Istituto Superiore di Sanità, Ist. Naz. di Fisica Nucl. (INFN), Viale Regina Elena 299, I-00161 ROMA.
 Dipartimento di Fisica, Università di Roma II and INFN, Tor Vergata, I-00173 ROMA.
³⁰⁾Facultad de Ciencias, Universidad de Santander, av. de los Castros, E - 39005 SANTANDER.
³¹⁾Inst. for High Energy Physics, P.O. Box 35, Protvino, SERPUKHOV (Moscow Region), U.R.S.S.
³²⁾Institute of Physics, University of Stockholm, Vanadisvägen 9, S-113 46 STOCKHOLM.
³³⁾Dipartimento di Fisica Sperimentale, Università di Torino and INFN, Via P. Giuria 1, I-10125 TORINO.
³⁴⁾Dipartimento di Fisica, Università di Trieste and INFN, Via A. Valerio 2, I-34127 TRIESTE.
 Istituto di Fisica, Università di Udine, I-33100 UDINE.
³⁵⁾Department of Radiation Sciences, University of Uppsala, P.O. Box 535, S-751 21 UPPSALA.
³⁶⁾Inst. de Fisica Corpuscular IFIC, Centro Mixto Univ. de Valencia-CSIC, Avda. Dr. Moliner 50, E-46100 BURJASSOT (Valencia).
³⁷⁾Institut für Hochenergiephysik, Österreich Akad. d. Wissensch., Nikolsdorfergasse 18, A-1050 VIENNE.
³⁸⁾Inst. Nuclear Studies and, University of Warsaw, Ul. Hoza 69, PL-00681 WARSZAWA.
³⁹⁾Fachbereich Physik, University of Wuppertal, Postfach 100 127, D-5600 WUPPERTAL 1.

1 Introduction

The Higgs mechanism [1], which is still not established, is an essential ingredient of the Standard Model [2]. In its minimal version the Standard Model predicts the existence of a neutral scalar Higgs particle, H^0 , and its couplings but the model gives no limits on its mass.

The coupling of the H^0 to fermions is proportional to their mass and that to bosons to their mass squared. Searches for the H^0 in the decay of relatively light bosons like π , K , B and Υ [3,4,5] are rather dependent on the assumptions used but tend to exclude a very light Higgs boson. Searches in Z^0 decays at LEP can determine a lower mass bound for the Higgs particle without using any limiting assumptions. Indeed the first results from LEP [6,7] support the exclusion of a light Higgs particle. In this note we report the first limits from the DELPHI detector on the Bjorken bremsstrahlung process [8]:

$$e^+e^- \rightarrow H^0 + Z^{*0} \rightarrow H^0 + f\bar{f} \quad (1)$$

where the off mass shell Z^{*0} decays into a pair of fermions.

Our search covers final states with $Z^{*0} \rightarrow e^+e^-$, $\mu^+\mu^-$, $\tau^+\tau^-$, $\nu\bar{\nu}$ and (at low H^0 masses) $q\bar{q}$.

For H^0 masses above 20 GeV/ c^2 the production cross section is too small to be detectable in these data. The present search is therefore optimized and restricted to the H^0 mass region below 20 GeV/ c^2 .

2 The DELPHI Detector

DELPHI is a general purpose detector equipped with track detectors, electromagnetic and hadron calorimeters and muon detectors. Details of the detector can be found in Refs. [9,10]. In the present analysis we use the following main components of DELPHI:

- The Inner Detector (ID), the Time Projection Chamber (TPC) and the Outer Detector (OD) for reconstruction of charged tracks.
- The High density Projection Chamber (HPC) to distinguish electrons from minimum ionizing particles. Each HPC module is equipped with one layer of trigger scintillators.
- The Barrel Muon Chambers (MUB) and the Hadron Calorimeter (HAC) for muon identification.

- The Time Of Flight counters (TOF) for triggering.
- The Small Angle Tagger (SAT) to veto large energy depositions at small angles.

The trigger is based on information from ID, OD, HPC and TOF. For trigger purposes the HPC, TOF and OD are each split into four quadrants around the beams and the the HPC and TOF are further split longitudinally into two halves on either side of the interaction point. Thus there are eight HPC sectors, eight TOF sectors, four OD sectors and one ID sector. The relevant trigger for this analysis was an OR of the following trigger components

- 2 or more HPC sectors,
- 3 or more TOF sectors,
- 1 or more HPC sector and 1 or more TOF sector,
- back to back TOF sectors and
- back to back ID and OD sectors in coincidence.

3 Monte Carlo Simulations and Standard Model Predictions

Samples of Monte Carlo events due to reaction (1) and to potential background processes were used to optimize the selection criteria and determine their efficiencies. The efficiencies for triggering the events were also determined by the same method.

The H^0 production processes were simulated using the DELPHI simulation program [11] with an $H^0 Z^{*0}$ generator [12]. For H^0 masses above 2 GeV/c^2 , the quark fragmentation was simulated using the LUND parton shower model (version 6.3) [13]. The same LUND parton shower model was used for simulating ordinary $q\bar{q}$ events to evaluate the backgrounds. For H^0 masses below 2 GeV/c^2 , exclusive 2-body channels were generated with relative weights following reference [14]. The simulated events were reconstructed with the standard DELPHI reconstruction program which was also used for the real events.

The expected cross sections for $Z^0 \rightarrow H^0 Z^{*0}$ within the Standard Model were estimated using the formalism of references [8,15]. Initial state radiative

corrections to first order were included and the effect of running coupling constants [16] was taken into account by using $\alpha = 1/128$ and $\sin^2 \theta_W = 0.2337$. The Z^0 mass and width were set at $91.2 \text{ GeV}/c^2$ and $2.5 \text{ GeV}/c^2$ respectively. Using the estimated cross section for $e^+e^- \rightarrow Z^0 \rightarrow \text{hadrons}$, the ratio $\sigma(e^+e^- \rightarrow Z^0 \rightarrow H^0 Z^{*0})/\sigma(e^+e^- \rightarrow Z^0 \rightarrow \text{hadrons})$ was determined as a function of the H^0 mass and the total center of mass energy. Summing over the number of hadronic Z^0 events at each LEP energy point, these cross section ratios were used to determine the expected number of H^0 events. The radiative corrections reduce the cross section ratio by 8% and 2% for H^0 masses of $3 \text{ GeV}/c^2$ and $10 \text{ GeV}/c^2$ respectively. Higher order radiative corrections are likely to decrease this effect, making our estimated number of events slightly conservative.

4 Data Sample

This analysis is based on some 13000 Z^0 decays, corresponding to a total integrated luminosity of about 650 nb^{-1} , provided by the LEP machine and recorded in DELPHI during the energy scans around the Z^0 peak. The overall efficiency to trigger and to reconstruct a hadronic Z^0 decay was found to be $(92.1 \pm 1.1)\%$ [10]. In these initial periods of running, some of the detector components were not always working properly. The data for a given channel have been selected so that the detector meets the minimum requirement for that channel, thus reducing the used luminosity to about 530 nb^{-1} . For the inclusive charged lepton and $H^0 \mu^+ \mu^-$ channels we used 10467 events with TPC and OD fully working. For the exclusive $H^0 e^+ e^-$ channel we used 9705 events with TPC and HPC fully working. For the $H^0 \nu \bar{\nu}$ and $H^0 q \bar{q}$ channels we used 10948 events with full TPC data. In the first part of running, corresponding to about one third of the data, the magnetic field was 0.7 T. In the remainder it was 1.2 T. In the present analysis only the barrel region of the DELPHI detector was used, covering polar angles, θ , between 40° and 140° .

5 H^0 and $Z^{*0} \rightarrow$ Neutrino Pairs

The Z^0 decay into a pair of neutrinos has about a factor of three larger branching ratio than the electron and muon pair branching ratios together. The characteristic signature for the $H^0 \nu \bar{\nu}$ channel is a large amount of missing energy and, particularly for relatively small H^0 mass (below $10 \text{ GeV}/c^2$), a

monojet topology. The main background processes, having a large fraction of undetected energy, are the beam-gas or beam-wall interactions and the two-photon process with undetected e^+e^- . Ordinary $e^+e^- \rightarrow Z^0 \rightarrow q\bar{q}$ events contribute to the background when energy is lost because of semileptonic decays or inefficiencies.

The simulated total trigger efficiency versus H^0 mass is presented on Fig. 1. The errors take into account the possible variations of the HPC trigger threshold and the TOF counter inefficiencies. The trigger components most sensitive to the neutrino channel are (a) one or more HPC sectors with one or more TOF sectors and (b) back to back OD sectors with ID in coincidence. The low trigger efficiency for low H^0 masses is due to the relatively high energy threshold in HPC (about 2 GeV) and the lack of back to back event topology in the signal.

The event selection relies exclusively on charged particles, the main emphasis being on the topological characteristics of the event, such as sphericity, monojet-type etc. Some of the cuts varied with the total invariant mass of the observed charged particles. The selection criteria, optimized for an H^0 mass in the interval 1 to 20 GeV/c² were:

- The total multiplicity of charged particles should be 2 or more.
- The $|\cos \theta|$ of the total event sphericity axis should be below 0.8.
- The sphericity calculated in the rest frame of the charged particles should exceed a value between 0.025 and 0.1, depending on the total invariant mass of the charged particles.
- The cosine of the angle of any charged particle in the event with respect to the total momentum vector should be above a value between -0.5 and 0.4, depending on the total invariant mass of the charged particles.
- The total transverse momentum of charged particles should be above a value between 1.5 and 6.5 GeV/c, depending on the total invariant mass of the charged particles.
- Clustered energy depositions in each SAT calorimeter should be below 10 GeV.

The simulated detection efficiency (trigger times selection efficiency) for the $H^0\nu\bar{\nu}$ channel is shown in Fig. 2 as a function of the H^0 mass.

Applying these selection criteria to our data sample 3 events remained all having a total mass of charged particles above $40 \text{ GeV}/c^2$. This is compatible with results from Monte Carlo studies of background from hadronic Z^0 decays which predict between one and two events one of them above $40 \text{ GeV}/c^2$. Thus no events were found in the data fulfilling the selection criteria with masses below $20 \text{ GeV}/c^2$, the region to which this study is restricted.

6 H^0 and $Z^{*0} \rightarrow$ Charged Leptons

The reaction $Z \rightarrow Z^{*0} H^0$ with a subsequent Z^{*0} decay to a fermion pair presents a simple and characteristic signature for the two cases:

$$e^+e^- \rightarrow H^0 e^+e^- \quad (2)$$

$$e^+e^- \rightarrow H^0 \mu^+\mu^- \quad (3)$$

They give rise to distinct topologies with two high energy almost back to back electrons or muons isolated from the H^0 decay products.

Two approaches have been used to search for $H^0 e^+e^-$ and $H^0 \mu^+\mu^-$ events. One approach (section 6.1) relies on measured angles and momenta without requiring any lepton identification. This method also detects a fraction of the channel $e^+e^- \rightarrow H^0 \tau^+\tau^-$ which is also included in our analysis. The other approach (section 6.2) requires the identification of one electron or muon and a second high energy particle compatible with being of the same type as the identified lepton, but of opposite charge.

6.1 Inclusive Method

The first approach relies on the isolation of the leptons from the Z^{*0} decay rather than on their identification. At least four charged particles are required, at least two of them having momenta above $5 \text{ GeV}/c$ and at least one of these making an angle larger than 20° with any other particle above $0.1 \text{ GeV}/c$ (isolation angle). The isolated particle is further required to have an opening angle of more than 90° with another particle with momentum above $5 \text{ GeV}/c$.

This tagging yielded a sample of 398 events. We then further

- required the two particles with momentum above $5 \text{ GeV}/c$ to have: one an isolation angle above 30° and the other above 10° ,
- required the total energy in the event to be greater than 30 GeV and the longitudinal momentum balance to be better than $20 \text{ GeV}/c$ and

- rejected events with a single particle opposite to a 40° cone containing all the other particles.

The last two of these cuts reject beam gas, radiative lepton pair and τ -pair events. After these cuts 12 events remained, compatible with 18 events expected from the background. In all these events, the invariant mass of the system excluding the two isolated particles was greater than $50 \text{ GeV}/c^2$. These events are therefore not of interest for the H^0 mass range below $20 \text{ GeV}/c^2$ to which this study is restricted.

Simulated events for different values of the H^0 mass were passed through the same selection criteria. The combined trigger, tagging and selection efficiency for this method is shown in Fig. 3.

No $H^0 Z^0$ candidates with H^0 mass below $20 \text{ GeV}/c^2$ remained after applying the cuts described in this section.

6.2 Exclusive Method

The second approach looks for channels with identified leptons. Candidates for the the electron channel (2) are tagged by demanding an electromagnetic energy deposition above 20 GeV and at least four charged particles detected in the TPC. This tagging yielded a sample of 457 events. Next we require at least one identified electron. An electron is identified by a charged particle spatially correlated to an electromagnetic shower with energy above 5 GeV . In addition there should either be a second identified electron of opposite charge, or a particle with momentum above $5 \text{ GeV}/c$ pointing towards a dead region in the electromagnetic calorimeter (HPC), or an electromagnetic deposition above 5 GeV matching a dead region in the TPC. Allowing for dead regions increases the selection efficiency by about a factor 1.25. One of the two selected electrons must be associated with the tagging shower. For events with charged multiplicity above five, the two electrons are required to be separated by at least 20° from the axes of all the jets reconstructed in the rest of the event. The jets were reconstructed using the LUND cluster algorithm [13] with default parameters. For events with four or five charged particles the two electrons are required to be separated from all the other charged particles by at least 25° .

For the exclusive muon channel (3) we used the same sample of events tagged for the inclusive lepton channel described above. A particle is assumed to be a muon if it is associated with at least two hits in different muon chamber layers or if it is minimum ionizing in the hadronic calorimeters.

The efficiency for this identification is found to be about 80% from studies of real and simulated events. The events with two identified muons are further required to have an angle between the muons larger than 90° .

After applying these cuts, two events with four charged particles were left having a charged particle pair compatible with being due to photon conversion. This is compatible with an estimated background of three such events from radiative leptonic Z^0 decays. A cut removing very small opening angle charged particle pairs was introduced and included in the efficiency calculations.

Fig. 2 shows the combined trigger, tagging and selection efficiency for reactions (2) and (3) as a function of H^0 -mass. The relative errors indicated are the statistic and systematic errors added in quadrature. They amount to about 5% in the centre of the mass range considered and 10% at the lower end.

No $H^0 Z^{*0}$ candidates were left in the data samples after applying the selections described in this section.

7 H^0 and $Z^{*0} \rightarrow$ hadrons

For the leptonic channels discussed above the efficiencies become low for an H^0 mass below $1 \text{ GeV}/c^2$ due to the cuts imposed and the trigger performance. In the mass region below $2 \text{ GeV}/c^2$ the H^0 total branching ratio into a pair of muons, charged pions and kaons is substantial, which leads to the possibility of identifying the $H^0 q\bar{q}$ channel. For this mass region there are considerable theoretical uncertainties in the prediction of H^0 branching ratios [17] for which we use ref. [14]. However, we are only sensitive to the total branching into two charged particles for which the most conservative estimate is always taken. In particular, for masses between threshold and $1 \text{ GeV}/c^2$, the two pions channel is assumed to dominate over the two muons one. A light H^0 decaying into two particles would lead to an event topology with at least three jets. Two of these come from the decay of the off mass shell Z^{*0} and a third jet from the H^0 . The abundant background coming from normal hadronic events is reduced by requiring:

- The total charged particle energy must be larger than 40 GeV.
- At least three jets, using the LUND cluster algorithm [13] with default parameters.

- The angle between the two most populated jets must exceed 120° .
- The least populated jet must have two to four charged particles, of which two and only two have momentum above $1 \text{ GeV}/c$.
- The ratio of the energies of these two candidate H^0 decay products must be below 5.5. This is equivalent to accepting a H^0 rest frame helicity angle from about 30° to 150° .
- The transverse momenta of the H^0 candidate with respect to all other jets must exceed $7 \text{ GeV}/c$.
- The angle between the H^0 candidate and any charged particle with an energy above 1 GeV must be larger than 40° .

After all cuts no candidate was left.

To calculate the H^0 detection efficiency, the selection criteria were applied to Monte Carlo samples of $H^0 q\bar{q}$ generated with H^0 in the mass range 0.2 to $2.0 \text{ GeV}/c^2$ and decaying into $\mu^+\mu^-$, $\pi^+\pi^-$ or K^+K^- . Using the branching ratios and the efficiencies for the different channels a global efficiency was calculated as a function of the H^0 mass. The results are shown in Fig. 4. The errors are the systematic and statistical errors added in quadrature. Systematic errors were estimated to be of the order 5%, smaller than the statistical ones. The detection efficiencies for the channels $H^0 \rightarrow \mu^+\mu^-$, $\pi^+\pi^-$ and K^+K^- (when kinematically allowed) were found to be almost the same thus making the global efficiency insensitive to their relative branching ratios.

8 Results and Conclusions

The number of detected H^0 events expected within the minimal Standard Model (SM) as a function of the H^0 mass are shown in Fig. 5 for the hadronic channel and in Fig. 6 for the leptonic channels. They are calculated from the numbers of hadronic Z^0 events recorded at each LEP energy, the corresponding relative cross sections for $H^0 Z^{*0}$ production, and the detection efficiencies, as described above. Lines corresponding to 95% confidence level for the exclusion of a signal are also included. The error bars represent the systematic and statistical errors added in quadrature. In order to take systematic errors into account in a conservative way we have subtracted one standard deviation as indicated by the curves. For the $H^0 \mu^+\mu^-$ and $H^0 \tau^+\tau^-$ channels we used

the detection efficiency from the inclusive method and for the $H^0 e^+ e^-$ channel that from the exclusive method, ignoring the small increase in detection efficiency arising from combining the inclusive and exclusive method. Using the results from the hadronic Z^0 channels for H^0 masses below $1 \text{ GeV}/c^2$ and the results from leptonic channels for higher masses, we exclude a minimal Standard Model Higgs boson in the mass region between $210 \text{ MeV}/c^2$ and $14 \text{ GeV}/c^2$.

Acknowledgements

We are greatly indebted to our technical staffs and collaborators and funding agencies for their support in building the DELPHI detector and to the many members of LEP Division for the speedy commissioning and superb performance of the LEP machine.

References

- [1] P.W. Higgs, Phys. Lett. **12** (1964) 132, Phys. Rev. Lett. **13** (1964) 508 and Phys. Rev. **145** (1966) 1156;
F. Englert and R. Brout, Phys. Rev. Lett. **13** (1964) 321.
- [2] S.L. Glashow, Nucl. Phys. **22** (1961) 579;
S. Weinberg, Phys. Rev. Lett. **19** (1967) 1264;
A. Salam, Proc. Nobel Symposium, ed. N. Svartholm (Almqvist and Wiksells, Stockholm, 1968) 367.
- [3] S.J. Freedman et al., Phys. Rev. **52** (1984) 240;
I. Beltrani et al., Nucl. Phys. **A451** (1986) 679;
N. Baker et al., Phys. Rev. Lett. **59** (1987) 2832;
P. Franzini et al., CUSB collaboration, Phys. Rev. **D35** (1987) 2883;
S. Egli et al., Phys. Lett. **B222** (1989) 533.
- [4] P. Yepes, Phys. Lett. **B227** (1989) 182, **B229** (1989) 156 and
CERN-EP/90-02, to be published in Mod. Phys. Lett. A;
M. Davier and H. Nguyen Ngoc, Phys. Lett. **B229** (1989) 150;
A. Snyder et al., Phys. Lett. **B229** (1989) 169.
- [5] R.N. Cahn Rep. Prog. Phys. **52** (1989) 389;
M.S. Alam et al., CLEO collaboration, Phys. Rev. **D40** (1989) 712;
M.S. Atiya et al., preprint BNL/43212, PRINCETON-HEP 89-01, TRI-
PP-89-70;
G.D. Barr et al., Phys. Lett. **235** (1990) 356.
- [6] ALEPH Collaboration: D. Decamp et al., Phys. Lett. **B236** (1990) 233;
and
CERN-EP/90-16 submitted to Phys. Lett. B.
- [7] OPAL Collaboration: M.Z. Akrawy et al., Phys. Lett. **B236** (1990) 224.
- [8] J.D. Bjorken SLAC-198 (1977);
J. Finjord, Phys. Scripta **21** (1980) 143. .
- [9] DELPHI Collaboration: P. Aarnio et al., Phys. Lett. **B231** (1989) 539.
- [10] DELPHI Collaboration: P. Abreu et al., CERN/EP 90-32, to be published in Phys. Lett. B.

- [11] DELPHI 89-67 PROG 142
DELPHI 89-68 PROG 143.
- [12] G. Ekspong and K. Hultqvist, University of Stockholm, USIP Report 5 (1982);
B. van Eijk, DELPHI 83-84.
- [13] T. Sjöstrand, Comp. Phys. Comm. **27** (1982) 243; **28** (1983)229;
T. Sjöstrand and M. Bengtsson, Comp. Phys. Comm. **43** (1987) 367.
- [14] M. Voloshin and V Zakharov, Phys. Rev. Lett. **45** (1980) 688;
M. Voloshin, Sov. J. Phys. **44** (**3**) (1986) 478;
S. Raby and G.B. West, Phys. Rev. **D38** (1988) 3488.
- [15] F.A. Berends and R. Kleiss, Nucl. Phys. **B260** (1985) 32.
- [16] D.C. Kennedy and B.W. Lynn, Nucl. Phys. **B322** (1989) 1;
M. Consoli et al., Z Physics at LEP1, CERN 89-08 Vol. 1, page 7.
- [17] S. Dawson, J.F. Gunion, H.E. Haber and G.L. Kane, *The Physics of Higgs bosons: Higgs Hunter's Guide* (Addison-Wesley, Menlo Park, 1989).

Figure Caption

Figure 1: Trigger efficiency for $H^0\nu\bar{\nu}$ channel. The errors indicated are statistical.

Figure 2: Overall detection efficiencies for charged and neutral lepton channels determined by the exclusive method. The error bars represent the systematic and statistical errors added in quadrature.

Figure 3: Overall detection efficiencies for charged lepton channels determined by the inclusive method. The error bars represent the systematic and statistical errors added in quadrature.

Figure 4: Overall detection efficiency for the $H^0q\bar{q}$ channel. The error bars represent the systematic and statistical errors added in quadrature.

Figure 5: Expected number of observed events in the $H^0q\bar{q}$ channel as predicted by the Standard Model (SM). The error bars represent the systematic and statistical errors added in quadrature. The 95% confidence level for the exclusion of a signal is indicated by the dashed line. The full line is drawn subtracting one standard deviation in order to make a conservative estimate of the excluded H^0 mass range.

Figure 6: Expected numbers of observed events in the $H^0e^+e^-$, $H^0\mu^+\mu^-$ and $H^0\tau^+\tau^-$ channels as predicted by the Standard Model (SM). The error bars represent the systematic and statistical errors added in quadrature. The 95% confidence level for the exclusion of a signal is indicated by the dashed line. The full line for the total number of expected events is drawn subtracting one standard deviation in order to make a conservative estimate of the excluded H^0 mass range.

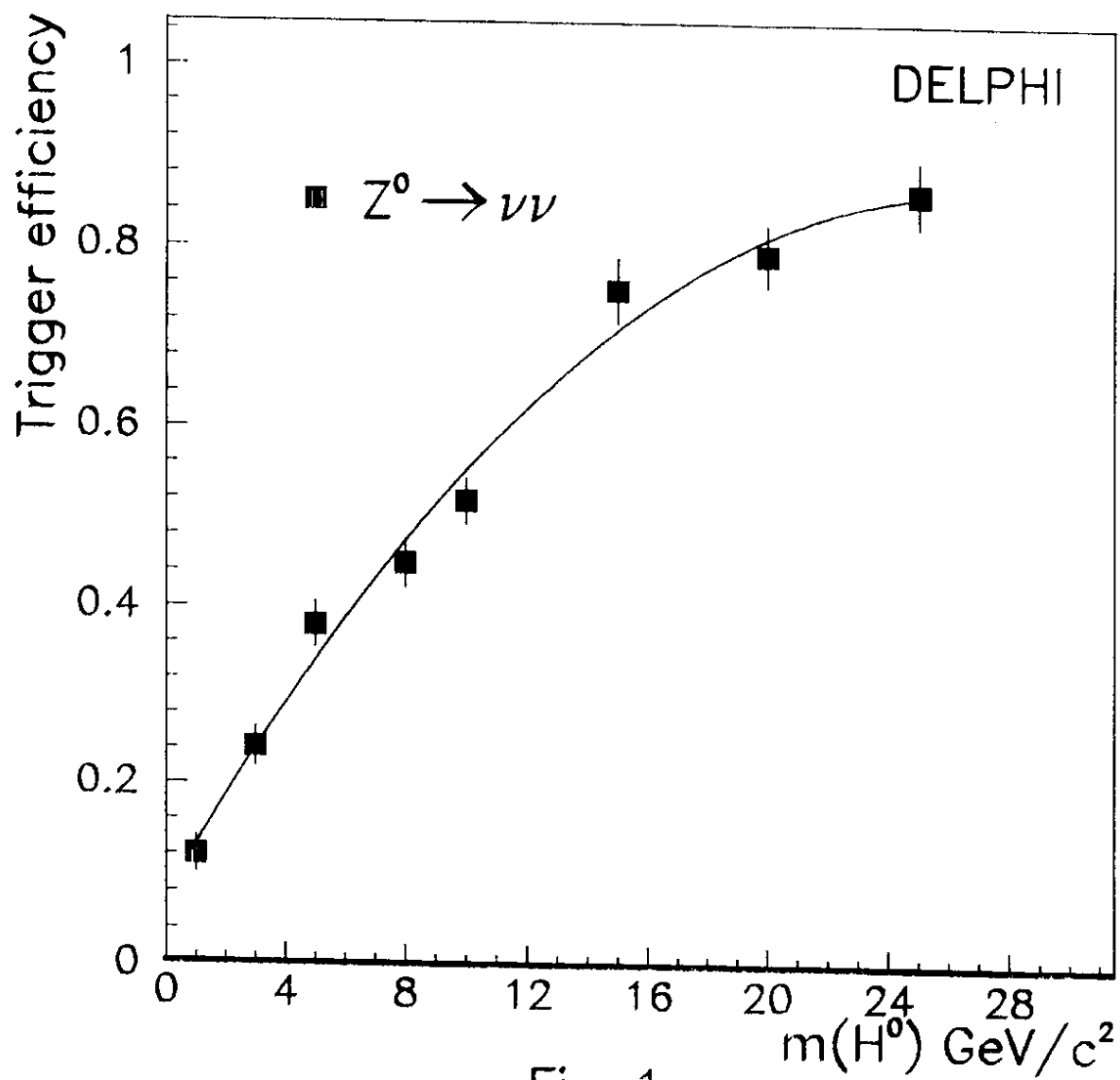


Fig. 1

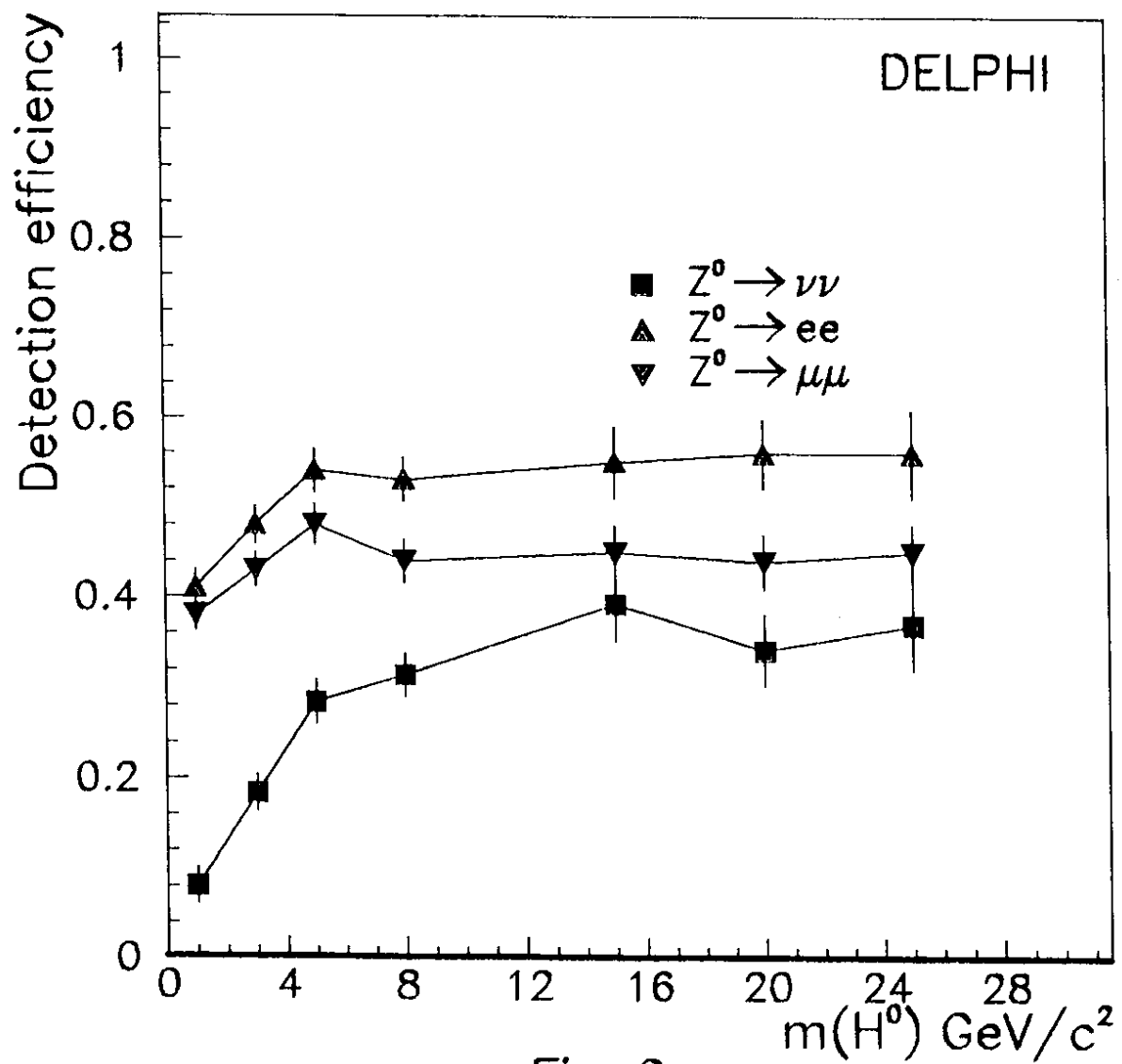


Fig. 2

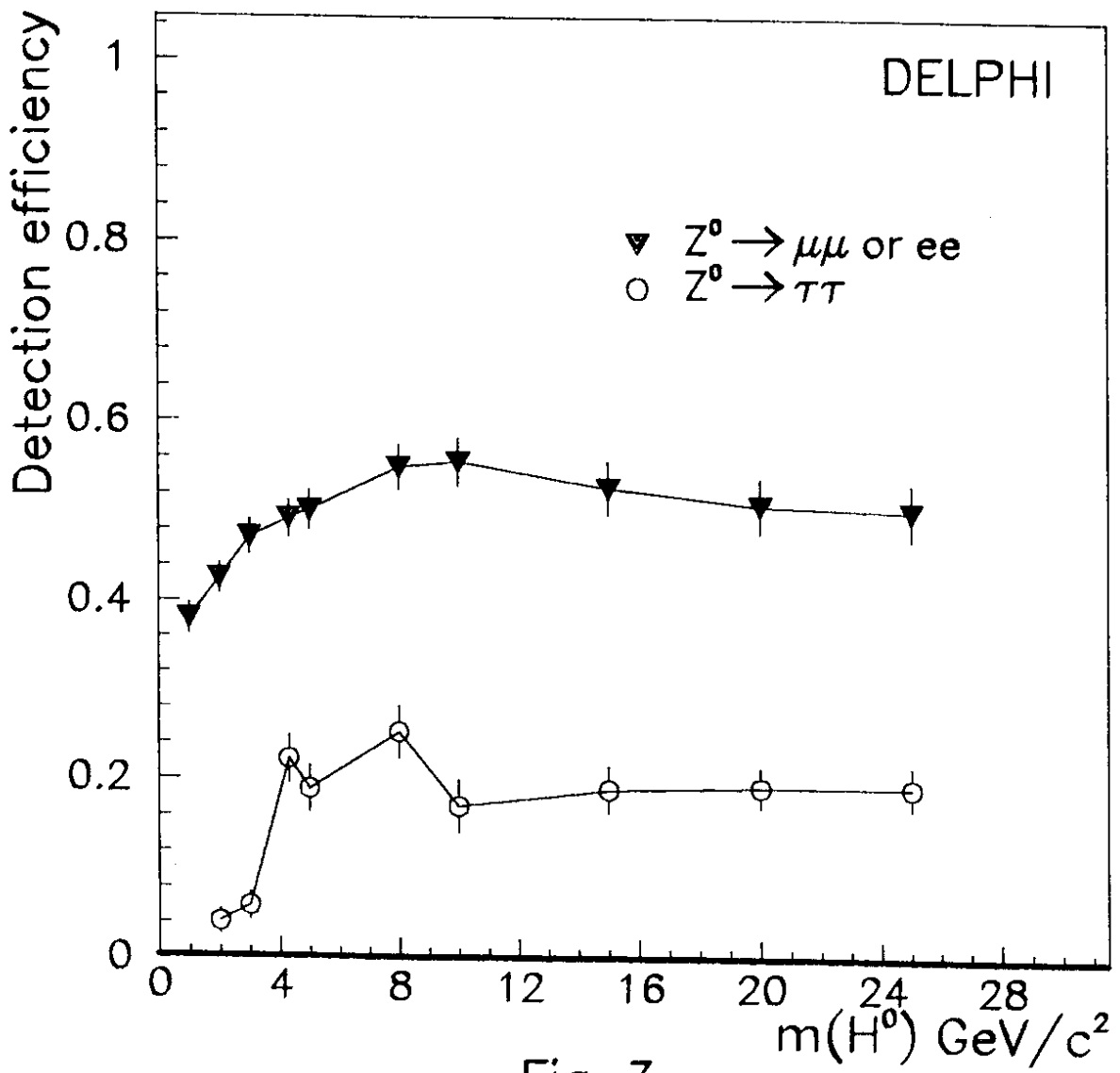
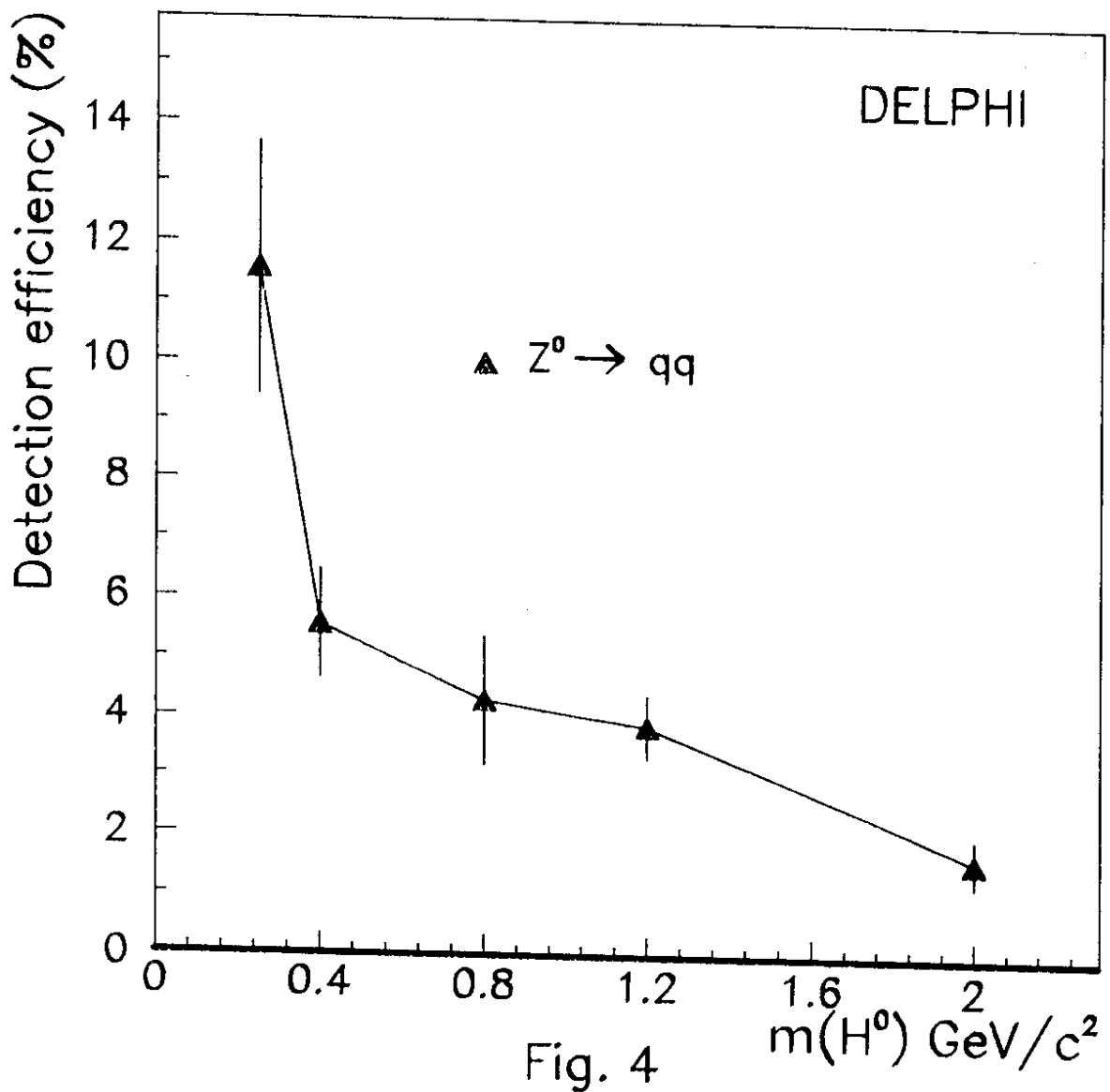


Fig. 3



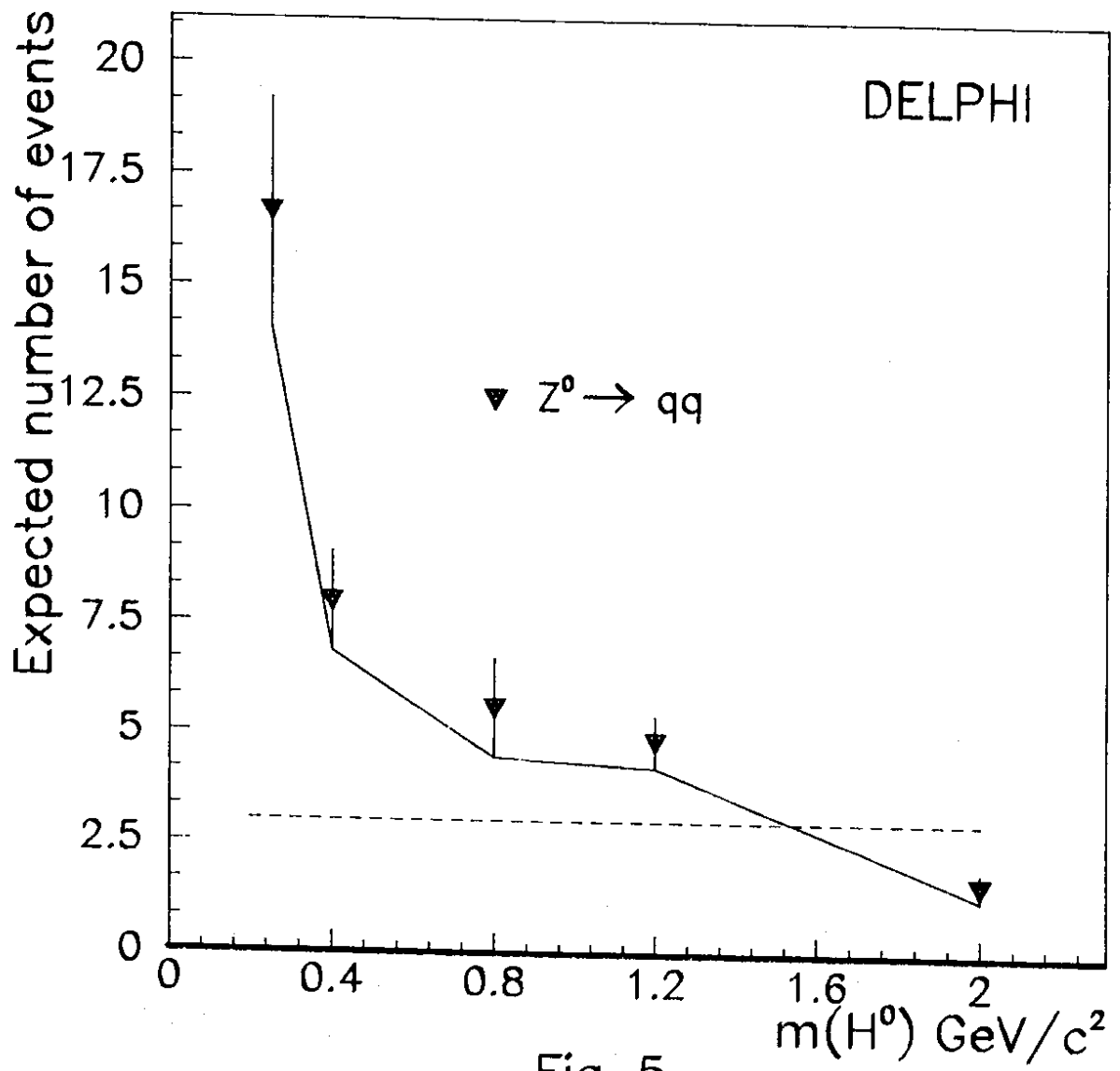


Fig. 5

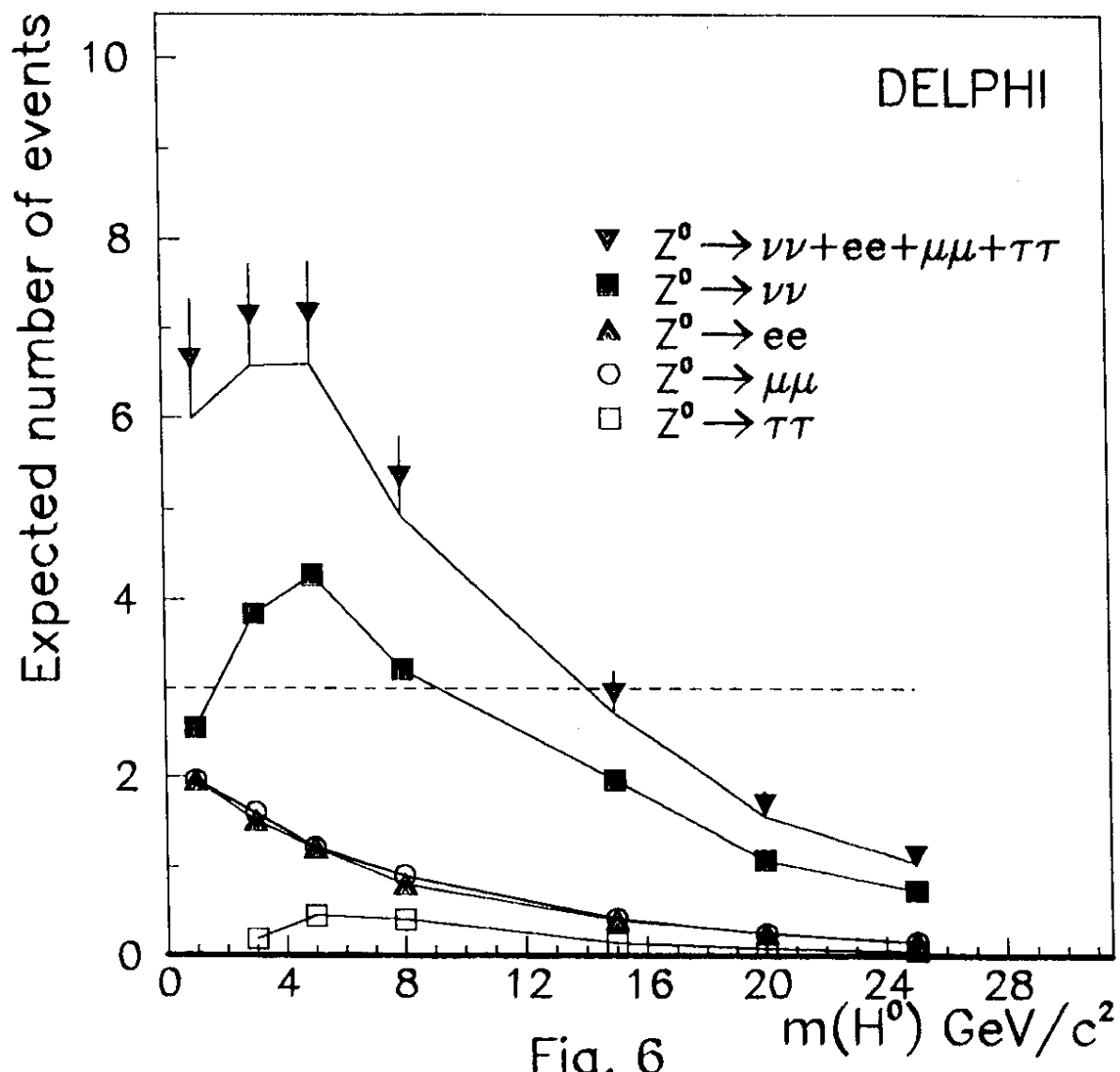


Fig. 6